Identification of Protein Changes in The Urine of Hypothyroid Patients Treated with Thyroxine Using Proteomics Approach

Afshan Masood
king saud university
Hicham Benabdelkamel (hbenabdelkamel@ksu.edu.sa)
King Saud Medical City https://orcid.org/0000-0001-9745-2959
Anwar A Jammah
king saud university
Aishah A Ekhzaimy
king saud university
Assim A Alfadda
king saud university

Research

Keywords: Hypothyroidism, Urine proteomics, 2D-DIGE, L-thyroxine treatment, Thyroglobulin metabolism.

Posted Date: March 5th, 2020

DOI: https://doi.org/10.21203/rs.3.rs-16161/v1

Version of Record: A version of this preprint was published at ACS Omega on January 13th, 2021. See the published version at https://doi.org/10.1021/acsomega.0c05686.

Abstract

Background The thyroid gland and thyroid hormones control a multitude of homeostatic functions including the functions kidney related to fluid and electrolyte balance and formation of urine. In the present study we aimed to define changes in the urinary proteome characterizing alterations in thyroid hormone status.

Methods An untargeted proteomic approach with network analysis was used to study 9 age-matched subjects with newly diagnosed overt hypothyroidism. Urine was collected from subjects pre and post L-thyroxine treatment. Proteome analysis was performed using two-dimensional difference in gel electrophoresis coupled with mass spectrometry.

Results 42 proteins were found to have significant differential abundance (≥1.5-fold change, ANOVA, $p \leq 0.05$). 28 proteins were upregulated and 14 proteins were downregulated in the hypothyroid compared to the euthyroid state. The differentially abundant proteins investigated by Ingenuity Pathway Analysis showed involvement of signaling pathways related to MAPK Kinase, VEGF, Pi3 Kinase/Akt, Pkc, and nvolvement of pathway related to amino acid metabolism, molecular transport, small molecule biochemistry.

Conclusions The differentially abundant proteins identified revealed their involvement in regulating TH and Tg metabolism. The alterations in levels of identified proteins in indicate a compensatory increase in the regulation of Tg to increase circulating TH levels in the hypothyroid state.

Background

The thyroid gland is the master controller of multitude of homeostatic functions and nearly all the physiological and metabolic activities of the human body. A strong interrelationship is also known to exist between the thyroid hormones and the kidney due to their entwined interactions including the control of fluid and electrolyte balance. Aside from this, the thyroid being a primary endocrine organ plays an important role in kidney growth and function [1]. Thyroid dysfunction causes significant changes in kidney function and affects physiology of the kidney, kidney structure, renal blood flow, glomerular filtration rate (GFR), tubular function, metabolism of water and electrolytes. This is because Kidneys in turn play a crucial role in metabolism and elimination of thyroid hormone (TH) and any diseases there in are accompanied by changes in synthesis, secretion, metabolism, and elimination of thyroid hormones (TH). The alterations in the activity of thyroid hormones are reflected by the presence of by-products of these metabolisms and energy regulating pathways that spill from the tissues into the circulation which are ultimately filtered out by the kidney. Hypothyroidism, characterized by a low thyroxine level, results in reduction of GFR and results in increased glomerular capillary permeability to proteins. The consequent proteinuria often precedes the reduction in GFR in hypothyroidism. Conversely patients with chronic kidney disease (CKD) and those with nephrotic syndrome are also known to present with hypothyroidism and/or subclinical hypothyroidism [2, 3].

The filtering capacity of the kidneys depends on the activity of the TH which in turn effects the filtering capacity and the formation of urine. The urinary proteins reflect changes in protein concentrations arising from the circulation in addition to the proteins that arise from the glomerulus, renal tubules, and the urinary tract. In healthy individuals it has shown that 70% of the urinary proteins originate from the kidney and the urinary tract, whereas the remaining 30% represents proteins filtered by the glomerulus [4]. Being an ultrafiltrate of the plasma, the urine is less complex than plasma and a more appropriate biological fluid to study pathological processes arising from either the kidney, urogenital tract and even from systemic diseases [2, 3]. This is also seen in cases of different systemic diseases in which proteolytic fragments generated from small circulating proteins peptides and vesicles pass through the glomerulus and change the urinary proteome.

Whole-expression proteomics or proteomic profiling, using high-throughput proteomic technologies such as two-dimensional difference in gel electrophoresis (2D-DIGE), allows determination of differences in the proteomes between normal and disease conditions. The techniques is advantageous over the traditional two-dimensional polyacrylamide gel electrophoresis as the fluorescence pre-labeling of proteins increases the sensitivity and detection of low abundance proteins, and the use of pooled internal standard allows for quatitative accuracy and reduces gel-to-gel variability [6].

Urine proteomics that employs a noninvasive and simple mode of sampling, makes it very convenient source of diagnostic biological fluid with a large number of proteins whose identification has improved over the years. [7, 8] This is documented in the human urine PeptideAtlas database which contains a total of 23,739 peptides corresponding to 2487 proteins. Several authors including our group have utilised the urine proteomic approach for analyses of varying diseases that include both renal and non-renal systemic conditions [5, 9–13] and for identification of biomarkers of cancer[14–18]. The effect of L-thyroxine on the plasma proteins before and after treatment was studied earlier by our group and others to identify the changes in the plasma proteome. No studies to date have looked at the urinary profile of these patients. The influence of thyroid dysfunction on the urinary proteome and urine was assessed almost entirely using rodent models. Even if these studies undoubtedly added to our understanding of TH action on metabolism, translation of these results to humans is still missing [19].

In the present study we aimed to look at the urinary profiles of the patients with hypothyroidism before and after treatment with L-thyroxine to identify the proteins that are changed between the disease and normal states using a quantitative 2D-DIGE followed by matrix assisted laser desorption and ionization time of flight (MALDI TOF) mass spectrometry (MS) identification. A detailed knowledge of all these interactions will help in the understanding of the disease pathophysiology and also help in optimal management of the patients.

Methods

Ethical approval and consent to participate

All procedures performed in the study involving human participants were in accordance with the ethical standards of the declaration of Helsinki and the universal ICH-GCP guidelines. The study protocol was approved by the Institutional Review Board, College of Medicine, King Saud University Hospital (No E-10-172). Written, informed consent was obtained from all participants.

Study design and participant selection

We studied 9 patients (6 females and 3 males, age: 39 +_ 12.9 years) years who were referred to our endocrine outpatient clinic at KKUH with newly diagnosed overt hypothyroidism. Blood samples were obtained from each patient after 10 hrs fasting and before starting thyroxine (pre-treatment sample). The sample size was determined by carrying out a power analysis using the Progenesis same spots nonlinear dynamics statistical software for determination of minimum number of required biological replicate (Additional File 1: Figure S1). Hypothyroidism was defined as a TSH level higher than 10 mIU/L and FT4 levels lower than 12 pmol/L. Samples were obtained from each patient at two time points: pretreatment samples (hypothyroid) were collected before starting treatment and the post-treatment samples (euthyroid) were obtained from those with TSH level normalized after treatment with the appropriate dose of L-thyroxine treated 6 weeks duration or until the thyroid hormones normalized to euthyroid levels. None of the patients recruited in the study had a history of hypertension, diabetes mellitus, inflammatory or other autoimmune. Blood samples were collected after a standard 10 h fast by venipuncture into EDTA-coated tubes and plasma was obtained by centrifugation (15 min, 3000 × g), then was aliquoted and stored in multiple aliquots at −80°C until analysis [20].

Urine collection and protein extraction

Midstream Spot urine samples (50– 100 mL) were obtain from participants after a standard 10 h fasting in a clean catch specimen into a sterile urine container and immediately transported on ice to prevent microbe contamination and proteolysis. Urinary protein, urinary infection, urinary sugar, and occult blood was checked using urine test strip (Combur10Test, Roche).

The samples were then processed and insoluble materials were removed by centrifugation at 2,000 × *g* (4,000 rpm) at 4°C for 10 minutes, within 30 minutes of collection, to prevent protein release from these artifacts. The supernatants were carefully removed and frozen at −80°C in 2 mL aliquots for long-term storage. Proteins were isolated from the urine samples as described previously [21]. The protein pellets were solubilized in labeling buffer (7 M Urea, 2 M Thiourea, 30 mM Tris–HCl and 4% CHAPS, pH 8.5). Insoluble material was pelleted by centrifugation (12,000 ×g, room temperature, 5 minutes), and protein concentrations were determined in triplicate using the 2D-Quant kit (GE Healthcare, USA).

2D–DIGE and MALDI TOF/TOF MS analysis

DIGE analysis was performed to determine differentially expressed proteins between the hypothyroid Vs Euthyroid groups as described [20]. Briefly, Proteins extracted (50ug) from each sample were labeled with either Cy3 or Cy5, respectively. Labeling was performed for 30 min on ice in the dark. Reactions were then

quenched by the addition of 1 uL of lysine (10 mM) for 10 min on ice in the dark. A mixture of equal amounts of protein isolated from each sample in the experiment was labeled with Cy2 and used as internal standard See Additional file 1: Table S1, Supporting Information. After 2D-DIGE, gels were scanned on the Typhoon 9410 scanner with Ettan DALT gel alignment guides using excitation/emission wavelengths specific for Cy2 (488/520 nm), Cy3 (532/580 nm), and Cy5 (633/670 nm). DIGE images were analyzed using Progenesis Same Spots v 3.3 software (Nonlinear Dynamics Ltd., UK) to quantify differential expression, independent direct comparisons were made between Hypothyroid and Euthyroid, and fold change and p-values were calculated using one-way ANOVA. All spots were pre-filtered and manually checked before applying the statistical criteria (ANOVA test, $p \leq 0.05$ and fold ≥ 1.5). Furthermore the spots showing statistical significance between the groups were manually excised and in-gel digestion with trypsin as described [5, 20] MALDI-MS(/MS) data were obtained using an UltraflexTerm time-of-flight (TOF) mass spectrometer equipped with a LIFT-MS/MS device (Bruker-Daltonics) instrument as described [5, 20, 22, 23] briefly The reflector voltage was set to 21 kV and the detector voltage to 17 kV. Peptide mass fingerprints (PMF) were calibrated against a standard (peptide calibration standard II, Bruker Daltonics). The PMFs were processed using Flex Analysis software (version 2.4, Bruker Daltonics). MS data were interpreted by using BioTools v3.2 (Bruker Daltonics) . The peptide masses were searched against the Mascot search algorithm (version 2.0.04 updated 09/05/2018; Matrix Science Ltd., UK). Identified proteins were accepted if they showed a Mascot score higher than 56 and $p < 0.05$. Detailed information about protein identification is provided in Additional File 1: Table S2.

Immunoblotting:

To independently confirm the findings of the 2D-DIGE studies, statistically significant proteins with differential abundance were selected and examined by immunoblotting. Monoclonal antibodies against transferrin (Mouse, Cat # SC-365871), retinol-binding protein (Mouse, Cat # SC-69795) and beta actin (goat, N-18, Cat # SC-1616), were purchased from Santa Cruz Biotechnology (Santa Cruz, USA). An equal amount of protein from each sample (50 µg) was separated by one-dimensional discontinuous slab gel electrophoresis (12% SDS-polyacrylamide gel). Proteins were electrotransferred to a Immobilon-P, polyvinylidene difluoride transfer membrane (PVDF, Millipore, USA) using a mini trans-blot electrotransfer cell (BioRad, USA). Following transfer, the membrane was stained with Ponceau-S to confirm the transfer efficiency. The membrane was then blocked (5% fat free milk (FFM) in Tris-buffered saline (TBS), 1 h, RT) and rinsed (3 changes of TBS-T in 10 mM Tris HCl, 150 mM NaCl, 0.1% Tween 20 buffer). Samples were then incubated with the specified primary antibodies (1:200 dilution) in blocking buffer. Blots were incubated with the appropriate IgG-HRP-conjugated secondary antibody, the immunoreactive bands detected by enhanced chemiluminescence (ECL, Thermo Scientific, USA), visualized by scanning with Fluorchem Q (Cell biosciences, USA) and digitalized using the image analysis software Alpha view Q 3.0 (Cell biosciences, USA).

Bioinformatic analysis: functional classification of proteins and pathway analysis

The successfully identified proteins were then uploaded into the IPA Software program (Ingenuity® Systems, http://www.ingenuity.com). The program helps in identifying the proteins and annotating them with related functions and pathways. The annotations are carried out by overlaying the proteins with their most significant networks and biochemical pathways from previous publications. The identified proteins were additionally classified into different categories according to their molecular function and the biological processes in which they are involved, this was accomplished by to the information in the Gene Ontology database (http://www.geneontology.org/).

Statistical analyses

The results on the biochemical parameters in the Hypothyroid and Euthyroid group were presented as mean ± SD, and significant differences between the mean values were assessed using Student's t-test. All statistical analyses were conducted using Graph Pad Prism software, version 5.0 for Windows (GraphPad Software, San Diego CA, USA).

Statistical Analyses for gel image analysis: raw gel images were uploaded into Progenesis “SameSpots” software (Nonlinear Dynamics. UK) and an automated spot detection method was performed. Three different experimental designs were set in Progenesis for spot detection. One design compared between the Hypothyroid and Euthyroid groups at each sample Automatic analysis was performed to detect all the spots in all the gels samples. Each selected spot was verified and manually edited if necessary. Normalized volumes were used to identify spots that were differentially expressed. A cut-off ratio greater than 1.5-fold was imposed Student’s t-test was used to calculate statistically significant differences between groups. $P < 0.05$ was considered statistically significant. A principal component analysis (PCA) of the log-transformed spot data was performed.

Results

Anthropometric and biochemical data

The parameters and biochemical data of the recruited patients are summarized in Table 1. As expected, statistically significant changes (p value < 0.001) in biochemical profile were noted for FT4 and TSH values after becoming euthyroid post treatment with L-thyroxine.

2D-DIGE analysis and identification of differentially expressed proteins

In this study, we evaluated differential protein expression in a pair-wise samples from nine hypothyroid and nine euthyroid urine samples (18 samples from nine gels) through analytical 2D- DIGE technique followed by statistical analysis using Progenesis software. For these nine pairs of biological replicates, the internal standard was composed of all 18 samples. A representative 2D-DIGE images for one pair of samples is shown in Fig.1 Cy3 (Euth) (A), Cy5 (Hypo) (B), and Cy2 (pooled internal standard) (C).

All gel images were matched, aligned and considered for analysis. We detected a total of 1100 matched protein spots present consistently in all individual gels. A total of 49 protein spots showed a significant

differential change in protein abundance (ANOVA test, $p \leq 0.05$ and fold-change ≥ 1.5) between the two groups. The spot patterns across all the 9 gels had high reproducibility permitting further analysis. In some cases, variants of the same protein were found at several locations on the gel. MALDI-TOF mass spectrometry found these 42 spots to be unique protein sequences which were matched to entries in the SWISS-PROT database by Mascot with high confidence scores (Fig. 2A, Additional file 1: Table S2). Peptide mass fingerprints (PMF) successfully identified 42 out of the 49 protein spots that is for 28 proteins out of 34 differential expressed up regulated protein spots; and 14 proteins out of 15 differential expressed down regulated protein spots (Fig.2B and 2C). Among 42 proteins identified 28 protein spots being up regulated and 14 being down regulated in hypothyroid compared to the euthyroid state (Fig.2A and Table 1). In Fig.2A, the arrow indicates the differentially abundant spots that are either decreased (Green arrow) or increased (Red arrow) between the groups, yellow spots represent proteins with the same isoelectric point, molecular weight, and nearly equal fluorescence intensity. We were not able to determine and pick all differential expressed protein spots on the Coomassie stained gel [22] . The significantly up regulated proteins in the hypothyroid state were identified as Serum albumin (up 1.9 fold, p =0.009), Serotransferrin (up 4.5 fold, p = 0.044), Huntingtin-interacting protein M (up 3.3 fold, p= 0.002), V-type proton ATPase subunit B, brain isoform (up 2.3 fold, p =0.006), Beta-1, 3-galactosyl-O-glycosyl-glycoprotein beta-1,6-N-acetylglucosaminyltransferase 3 (up 2.8 fold, p =0.028), E3 ubiquitin-protein ligase DCST1 (up 2.4 fold, p =0.014), Cathepsin D (up 2.5 fold, p =0.026), Putative E3 ubiquitin-protein ligase UBR7 (up 1.9 fold, p =0.008), Keratin, type I cytoskeletal 10 (up 1.5 fold, p =0.016), Probable E3 ubiquitin-protein ligase TRIML2 (up 1.5 fold, p =0.036), AN1-type zinc finger protein 6 (up 2.1 fold, p =0.0.38), Keratin, type II cytoskeletal 5 (up 1.6 fold, p =0.044), Protein AMBP (up 2.8 fold, p =0.021), Vesicular integral-membrane protein VIP36 (up 2.2 fold, p =0.018), Kininogen-1 (up 1.8 fold, p =0.0015), Cleft lip and palate transmembrane protein 1-like protein (up 1.7 fold, p =0.021), Zinc finger protein 839 (up 2.5 fold, p =0.026), Homogentisate 1,2-dioxygenase (up 1.6 fold, p =0.053), Protein OS-9 (up 1.9 fold, p =0.058), Retinol-binding protein 4 (up 1.9 fold, p =0.058). The significantly down regulated proteins in the hypothyroid state were identified as Kin of IRRE-like protein 3 (down 3 fold, p= 0.014), Phosphopantothenoylcysteine decarboxylase (down 2.3 fold, p= 0.021), Syntaxin-binding protein 6 (down 1.7 fold, p= 0.042), Aryl hydrocarbon receptor nuclear translocator 2 (down 2.1 fold, p= 0.04), GTPase HRas (down 2.2 fold, p= 0.05), Nesprin-1 (down 3.4fold, p= 0.04), Serine/arginine repetitive matrix protein 2 (down 2.6 fold, p= 0.006), Protein-glutamine gamma-glutamyltransferase Z (down 3.9 fold, p= 0.022), IgA-inducing protein homolog (down 2.1 fold, p= 0.023), A disintegrin and metalloproteinase with thrombospondin motifs 8 (down 1.9 fold, p= 0.042), Prefoldin subunit 6 (down 2.1 fold, p= 0.030). (Table 2, Additional file 1: Table S2).

Confirmation of changes in selected proteins by immunoblotting:

Key proteins found to be differentially abundant between the groups were selected for confirmatory testing by immunoblot analysis (Fig.3). The proteins targeted for confirmation included: Transferrin, and RBP. Immunoblots confirmed the significantly ($p \leq 0.05$) differential expression of these proteins in the human plasma collected from the hypothyroid state in comparison to the euthyroid state. Immunoblot data were normalized to the housekeeping protein □-actin (Fig. 3A-3B).

Mapping of protein-protein interaction networks

The protein-protein interaction analysis was also performed for all these 48 differentially regulated proteins using Ingenuity Pathway Analysis. Analysis revealed that among the 48, 13 proteins interact either directly or indirectly through proteins networks (Fig. 4A). The software computes a score based on the best fit obtained from the input data set of proteins and from the biological functions database, to generate a protein-protein interactions network. The generated network is preferentially enriched for proteins with specific and extensive interactions, the interacting proteins are represented as nodes and their biological relationships as a line. Based on the data 3 interaction networks were identified for the proteins exhibiting differential expression profiles. The highest scoring network (score = 26) (Fig. 3) incorporated 13 focus molecules. The proposed highest interaction network pathway related to Amino Acid Metabolism, Molecular Transport, Small Molecule Biochemistry. Only the top pathways are shown (Fig. 4A).

Canonical pathways enriched in the current dataset are shown in the Fig.4B. The three most interesting enriched canonical pathways included thyroid hormone biosynthesis (30 % overlap), LXR/RXR Activatio (4.1 % overlap), FXR/RXR Activatio (4 % overlap) and Acute Phase Response Signalin (2.8 % overlap). Details of the canonical pathways identified in this study are summarized in Additional file 1: Figure S2.

Principal component analysis (PCA)

The PCA were performed using Progenesis Same Spots software which is helpful to determine and visualise the samples coming from the hypothyroid and euthyroid states. The PCA was performed on all 62 spot features which exhibited statistically significant (ANOVA $p < 0.05$) changes in abundance, identified by MS, the analyses revealed that the 2 groups clustered distinctly from one another based on different urine proteins with 64% of variability (Fig. 5).

Subcellular and functional characterization of the differentially expressed proteins.

Following MS analysis, all successful 42 differentially abundant proteins identified between the hypothyroid and euthyroid, were subjected to functional classification using Gene Ontology (GO) terms using UniProtKB. The identified proteins were classified in order to gain more information about their location Fig.6A and the molecular function Fig. 6B in which they are involved. The dominant functional categories identified were binding protein (34%), enzyme (29%), transporter (22%), cytoskeletal (5%) protein and others (10%).

Discussion

The metabolic functioning of all tissues depends on the optimal levels of circulating TH that are under the tight regulatory and feedback control of the hypothalamo- pituitary thyroid axis through actions of throtropin(TSH) and Tg. The kidney, a target organ for TH and is also responsible for its metabolism and breakdown along with TSH and thyroglobulin (Tg). Urine, the terminal metabolite of the body produced by

the kidney reflects not only kidney function but also the overall metabolism of the body through the presence of urinary vesicles and exosomes [24]. There is a strong interrelationship between the kidney and the thyroid wherein thyroid dysfunction leads to changes in glomerular filtration and tubular absorption as seen in hypothyroidism, decreased TH levels are accompanied by an increased peripheral vascular resistance, reduced renal blood flow, decreased glomerular filtration, altered tubular function, hyponatremia, and an alteration of the ability for water excretion. In the present study, we compared the urinary proteomic profiles in patients with hypothyroidism, before and after treatment with levothyroxine using the 2D-DIGE and MALDI-TOF proteomics approach, to better understand of the differences in the overall metabolism observed between the hypothyroid and euthyroid states. We had previously carried out a similar untargeted plasma proteomic profiling in the same group of patients [20]. Overall, our results showed that a total of 42 proteins, with a > 1.5-fold statistically significant change (P = 0.05) in abundance between the two states were altered, of which 28 proteins were up regulated and 14 proteins were down regulated in the hypothyroid state compared to the euthyroid state. On grouping these proteins based on their biological processes to understand their roles, we found that they were involved in the regulation of processes related to (i) transport (ALB, TF, RBP4, ATP6V1B2, HRAS, KNG1, LMAN2, ARNT2). (i) acute phase response proteins (ALB, TF, AMBP, CTSD, GCNT3, KNG1, KRT10, KRT5,), (iv) generation of reactive oxygen species (ALB,TF, HRAS, KNG1,) (iii) proliferation of connective tissue cells (TF, CTSD, HRAS, KNG1, KRT10,) and (ii) endocytosis (ALB, TF, AMBP, ATP6V1B2 up, HRAS ,LMAN2 ,SYNE1). The proteins ALB, RBP, HRAS, CTSD, TF, KNG1 were found to participate in combination with other proteins in more than one metabolic processes and regulate different pathways.

Transport of the TH from its site of synthesis to the target organs mediated via the TH binding proteins is critical for its action. Eight proteins identified in the present study were involved in the transport of TH. The presence of a number of different transport proteins, with different binding capacities ensures a balanced source of bioavailable TH to the different organs and also acts as sensor mechanism which determines the extent of liberation and release.

We found an increase in the levels of human serum albumin (HSA) in the urinary proteome of the hypothyroid group in comparison the euthyroid. HSA is a 66.5 kD protein synthesized by the liver and associates with a wide variety of substances and hormones including circulating TH. HSA, a low-affinity but high-capacity thyroid hormone binding protein binds 10% of the circulating TH and prevents its filtration by the renal tissue [1, 25]. Albumin secretion in the urine, above 150 mg/dl, is considered pathological (proteinuria) and is reflective of different systemic diseases, such as hypertension, diabetes or more locally kidney diseases (for example: glomerulonephritis). Increased albumin in the proteome with no evidence of urinary microalbuminuria, has been documented in number of proteomic studies [5, 26]. The increase in the albumin levels may reflect an increase in the uptake of the thyroid hormones, increased binding to prevent renal loss and in maintaining a balanced supply to the peripheral tissues during lowered thyroxine circulation as is seen in hypothyroidism. We and others have previously reported the presence of increased albumin in post bariatric surgery and in metabolic unhealthy obesity [26]. Hypothyroid patients also present with low grade chronic inflammation [27] and the increased spots relating to albumin along with AMBP levels also point to increase APP response along with and increased

oxidative stress in the hypothyroid state. AMBP contains α1-microglobulin and Bikunin an important anti-inflammatory substance that modulates inflammatory events. Urinary α1-microglobulin indicates proximal tubular dysfunction and an increase in AMBP in hypothyroidism may serve to determine early tubular changes and as an increased anti-inflammatory response [28].

The protein spots relating to RBP which circulates as part of the latransthyretin and binds 20% of circulating TH [25] were also found to be significantly increased in the urinary proteome between the hypothyroid and euthyroid states. TTR is known to originate in the liver, but is also found in kidney cells, the choroid plexus, meninges, retina, placenta and pancreatic islet cells and fetal intestine [29]. RBP and TTR are known to have an intermediate binding affinity for TH [30]. They bind 80% of T4 and facilitates its transport to the brain through the blood brain barrier and the CSF wherein it constitutes up to 25% of the total protein. Owing to its low molecular weight, RBP (21-kDa) is freely filtered by the glomerulus with subsequent reabsorption and catabolization by the proximal tubule, making it a marker for tubular function. The binding of RBP to TTR was suggested to prevent extensive loss of the low molecular weight RBP through glomerular filtration. Recently, RBP4 levels have been reported to be elevated in insulin resistant subjects as well as in subjects with obesity and type 2 diabetes (T2DM) [31].

The protein spots relating to LMAN, a vesicular integral membrane type I transmembrane lectin, that plays an important role intracellular protein trafficking was found increased in our study. This protein is involved in the sorting, vesicle-mediated transport, early secretory pathway trafficking, endocytosis and quality control of high mannose type glycoproteins like thyroglobulin (Tg) and erythropoietin. LMAN is a component of the lipid microdomain raft machinery that are responsible for Tg transport to the apical surface and delivery to follicular lumen via raft pathway for secretory endocytosis [32]. Tg is a prohormone that is internalised and highly glycosylated under the influence of TSH in the ER and the golgi where it undergoes significant post translational modifications, conformational maturation and homodimerization before intracellular transport [33]. Mature Tg binds TH in the follicular thyroid cells and is stored as colloid. TSH induces exocytosis and exocytotic vesicles are accumulated in the most apical cell region after being transported on LMAN containing lipid protein microdomains. Increase in LMAN may indicate an attempt to increase Tg synthesis to increase the physiological levels of T4 in the thyrocytes and similarly for erythropoietin synthesis from the kidney.

Another multifunctional protein identified with significantly increased abundance in the urine proteome is transferrin, a metal cofactor involved in the transport of iron and is also required for an effective peripheral deiodination of T3 and for activity of the deiodinase enzyme that are also present in the kidney [20]. We found an increase in the abundance of protein spots relating to urinary transferrin in the hypothyroid state similar to our earlier study where we demonstrated an increased levels in the plasma. Lin et al., in their study in hepatoma cell lines (HepG2-TRa1), showed a direct induction of serotransferrin by T3 [29].

We also found a decrease in the abundance of SYNE 1 a nuclear envelope spectrin-repeat proteins that localise to multiple sub-cellular compartments. It behaves as an interconnecting protein that links the

nuclear lamina to the cytoskeleton, and regulates the endothelial shape and migration [34], functions as the intracellular scaffold to maintain the cellular structure and establishes nuclear-cytoskeletal connections. These connections importantly connect the nuclear metabolism to the cytoplasmic actions for regulation of proteins such as Tg. SYNE1 mutations may disrupt tissue specific nesprin scaffolds and explain the tissue specific nature of many nesprin-associated diseases, including laminopathies and related to tumour progression and decreased expression was reported in invasive cancers [35, 36].

Hypothyroidism often leads to an enlargement of the thyroid gland as a compensatory mechanism to overcome the decrease in the circulating TH and in response to an increased TSH in order to increase TH production. The increase in proliferation was supported by our proteins - TF, CTSD, HRAS, KNG1, KRT10, which are known to increase Tg endocytosis and proteolysis, were significantly differentially abundant between the hypothyroid and euthyroid state. These included CTSD, E3 ubiquitin-protein ligase DCST1, putative E3 ubiquitin-protein ligase UBR7, probable E3 ubiquitin-protein ligase TRIML2, protein OS-9. Tg plays a role in the thyroid hormogenesis by its degradation via endosomal lysosomal pathway by cysteine cathepsins (thiol proteases) and the ubiquitin dependant proteolytic pathways. CTSD itself and by activation of cathepsin B breaks down the covalently cross-linked Tg in the acidic enodsomal environment to release soluble Tg for T4 liberation and re-utilization [37, 38]. A similar association was identified in. Cath-D is also a key mediator of induced-apoptosis, essential role in the multiple steps of tumor progression, in stimulating cancer cell proliferation, fibroblast outgrowth and angiogenesis, as well as in inhibiting tumor apoptosis. CTSD expression was increased in human primary breast cancer, thyroid and skin cancers, and was found to be associated with an increased risk of metastasis and shorter survival [39, 40].

We identified an increase in the ubiquitin-proteasome system (UPS) proteins, which includes the E3 ubiquitin ligases involved in the ubiquitin dependant proteosomal degradation of Tg between the hypothyroid and euthyroid state. This included the tripartite motif (TRIM) proteins which are the largest subfamilies of E3 ubiquitin ligases and UBR7 whose dysregulation is associated with chromatin abnormalities, numerous diseases and cancers. UBR7 is also important for the maintenance of the epithelial state and inhibition of the plasticity of a cell.

Aryl hydrocarbon-receptor nuclear translocator (ARNT2) is a transcription factor expressed in nervous system and kidney that also functions as E3 ubiquitin ligase. ARNT2 has been shown to be involved in angiogenesis and nerve development of embryo [41] while mutations in the ARNT2 gene are known to causes hypopituitarism, post-natal microcephaly, visual and renal anomalies [42]. Jia et al showed that ARNT2 inhibits cell proliferation inactivating the AKT signaling pathway in cases of gastric cancer [41]. The increase in all the enzymes involved in the proteolysis, endocytosis aims to liberate TH from the Tg leading to their secretion in the circulation [43].

It is interesting to note that the urinary proteome in our study also identified the enzyme GCNT3 and TGM7 with an increased abundance in the hypothyroid group. These enzymes are responsible for post translational glycosylation of Tg and increasing the covalent cross-links between the Tg molecules to

increase its compaction within the thyrocyte [44]. Tg glycosylation is important for its correct folding and trafficking, iodination and TH synthesis [45]. Unglycosylated Tg has been shown to lose its ability to synthesize TH in both in vitro and invivo studies [43]. Protein OS-9 identified in our data set with an increased abundance is an additional participating enzyme of this pathway. It is well known that Tg is a highly glycosylated protein with extended mannose residues that are recognised by protein OS-9 containing mannose 6-phosphate receptor homology domains, were reported to be involved in ER quality control [46].

We found a significant decrease in abundance of Hras in the hypothyroid versus the euthyroid states. Hras is a member of the membrane-bound guanine nucleotide-binding proteins that function as signal transducers from cell membrane to nucleus for TH and other growth factor receptors. Besides the thyroid tissue, Hras is expressed in the kidney and is abundant in the distal collecting duct [47]. Ras interacts with multiple downstream effectors including PI3K and leads to the activation of MAPK kinases resulting in gene induction. The ultimate outcome is regulated induction of cell survival, growth and migration, proliferation, differentiation, adhesion, motility, and morphology [48]. Among their diverse biological functions, Ras poteins are known to regulate activities of ion channels and transporters. Mutations in the other RAS proteins have been identified in benign and malignant thyroid neoplasms,[49, 50] in primary cultures of human thyrocytes and in rat thyroid cell lines except for Hras whose increased oncogenic mutants levels in mice did not develop thyroid lesions [50]. Our results also demonstrated an increase in the cleft lip and palate transmembrane protein 1-like protein (CLPTM1L) that works in conjunction with the RAS proteins through the phosphoinositide 3-kinase (PI3 Kinase) pathway and is an essential molecule its signaling functions. James et al identified an overexpressed protein in human ovarian tumour cell lines that are resistant to cisplatin and in non-small cell lung cancer, where it protects tumour cells from genotoxic apoptosis [51].

The other proteins of interest identified in the study with increased abundance between the hypothyroid and euthyroid state were Zinc-finger proteins (ZNFs) and the keratins that are involved in several cellular processes with key role in development and differentiation, tumorigenesis, cancer progression and metastasis.

The biological significance of the identified proteins in our proteomic analysis was explored by IPA and the network pathway identified the highest scoring interaction network pathway related to amino acid metabolism, molecular transport, small molecule biochemistry. This is true considering the fact that TH are peptide hormones whose synthesis is dependant on the amino acid metabolism. The central nodes with the highest connectivity included the MAP kinase family p38MAPK, ERK1/2,Jnk), PI3 Kinase/Akt, protein kinase C, Nfkb and VEGF, reiterating the involvement of the identified proteins in pathways related to cell proliferation, inflammation, and endothelial function. The proteome analysis also points to the fact that there is a concerted action to increase the TH circulating levels through increase Tg synthesis in the hypothyroid state.

Conclusion

In conclusion, our comparative proteomics study using 2D-DIGE analysis of the urine proteome profile between the hypothyroid and the euthyroid states revealed significant changes in the proteins related to TH and Tg metabolism. The alterations in the different proteins identified in the study demonstrate a compensatory increase in the regulation of Tg as an attempt to increase its production to increase the circulating levels of TH in the hypothyroid state.

Abbreviations

TH Thyroid hormone

GFR Glomerular filtration rate

CKD Chronic kidney disease

UPS Ubiquitin-proteasome system

TRIM Tripartite motif

GTPase Guanosine triphosphate hydrolase

Declarations

Ethics approval and consent to participate

The study protocol was approved by the Institutional Review Board, College of Medicine, King Saud University Hospital (No E-10-172). Written, informed consent was obtained from all participants

Consent for publication

Not applicable.

Availability of data and materials

Complete list of proteins identified is available in Additional file 1: Table S2

Competing interests

The authors declare no competing interest

Funding

This work was funded by the National Plan for Science, Technology and Innovation (MAARIFAH), King Abdulaziz City for Science and Technology, Kingdom of Saudi Arabia (Project no. 13-MED 920-02).

Authors' contributions

HB, AM, and AAA conceived the idea and designed the study. AAJ, AAE and AAA, were involved in patient recruitment. HB, AM, performed the proteomics lab work. HB, AM and AAA did data analysis and wrote the manuscript. All authors have read and approved the final manuscript.

Acknowledgments

The National Plan for Science, Technology and Innovation (MAARIFAH), King Abdulaziz City for Science and Technology, Kingdom of Saudi Arabia (Project no. 13-MED 920-02).

References

1. Iglesias P, Diez JJ. Thyroid dysfunction and kidney disease. European journal of endocrinology. 2009;160(4):503-15.
2. Shin DH, Lee MJ, Kim SJ, Oh HJ, Kim HR, Han JH, et al. Preservation of renal function by thyroid hormone replacement therapy in chronic kidney disease patients with subclinical hypothyroidism. The Journal of clinical endocrinology and metabolism. 2012;97(8):2732-40.
3. Li LZ, Hu Y, Ai SL, Cheng L, Liu J, Morris E, et al. The relationship between thyroid dysfunction and nephrotic syndrome: a clinicopathological study. Scientific reports. 2019;9(1):6421.
4. Thongboonkerd V, Malasit P. Renal and urinary proteomics: current applications and challenges. Proteomics. 2005;5(4):1033-42.
5. Benabdelkamel H, Masood A, Okla M, Al-Naami MY, Alfadda AA. A Proteomics-Based Approach Reveals Differential Regulation of Urine Proteins between Metabolically Healthy and Unhealthy Obese Patients. International journal of molecular sciences. 2019;20(19).
6. Masood A, Benabdelkamel H, Alfadda AA. Obesity Proteomics: An Update on the Strategies and Tools Employed in the Study of Human Obesity. High-throughput. 2018;7(3).
7. Adachi J, Kumar C, Zhang Y, Olsen JV, Mann M. The human urinary proteome contains more than 1500 proteins, including a large proportion of membrane proteins. Genome biology. 2006;7(9):R80.
8. Marimuthu A, O'Meally RN, Chaerkady R, Subbannayya Y, Nanjappa V, Kumar P, et al. A comprehensive map of the human urinary proteome. Journal of proteome research. 2011;10(6):2734-43.
9. Zimmerli LU, Schiffer E, Zurbig P, Good DM, Kellmann M, Mouls L, et al. Urinary proteomic biomarkers in coronary artery disease. Molecular & cellular proteomics : MCP. 2008;7(2):290-8.
10. Neisius U, Koeck T, Mischak H, Rossi SH, Olson E, Carty DM, et al. Urine proteomics in the diagnosis of stable angina. BMC cardiovascular disorders. 2016;16:70.
11. Guo HX, Zhu YB, Wu CP, Zhong M, Hu SW. Potential urine biomarkers for gestational hypertension and preeclampsia. Molecular medicine reports. 2019;19(4):2463-70.
12. Zhang ZY, Nkuipou-Kenfack E, Staessen JA. Urinary Peptidomic Biomarker for Personalized Prevention and Treatment of Diastolic Left Ventricular Dysfunction. Proteomics Clinical applications. 2019;13(2):e1800174.

13. Kaburagi Y, Takahashi E, Kajio H, Yamashita S, Yamamoto-Honda R, Shiga T, et al. Urinary afamin levels are associated with the progression of diabetic nephropathy. Diabetes research and clinical practice. 2019;147:37-46.
14. Sandow JJ, Rainczuk A, Infusini G, Makanji M, Bilandzic M, Wilson AL, et al. Discovery and Validation of Novel Protein Biomarkers in Ovarian Cancer Patient Urine. Proteomics Clinical applications. 2018;12(3):e1700135.
15. Wu D, Ni J, Beretov J, Cozzi P, Willcox M, Wasinger V, et al. Urinary biomarkers in prostate cancer detection and monitoring progression. Critical reviews in oncology/hematology. 2017;118:15-26.
16. Papale M, Vocino G, Lucarelli G, Rutigliano M, Gigante M, Rocchetti MT, et al. Urinary RKIP/p-RKIP is a potential diagnostic and prognostic marker of clear cell renal cell carcinoma. Oncotarget. 2017;8(25):40412-24.
17. Wang W, Wang S, Zhang M. Identification of urine biomarkers associated with lung adenocarcinoma. Oncotarget. 2017;8(24):38517-29.
18. Gajbhiye A, Dabhi R, Taunk K, Vannuruswamy G, RoyChoudhury S, Adhav R, et al. Urinary proteome alterations in HER2 enriched breast cancer revealed by multipronged quantitative proteomics. Proteomics. 2016;16(17):2403-18.
19. Rhee CM. The interaction between thyroid and kidney disease: an overview of the evidence. Current opinion in endocrinology, diabetes, and obesity. 2016;23(5):407-15.
20. Alfadda AA, Benabdelkamel H, Masood A, Jammah AA, Ekhzaimy AA. Differences in the Plasma Proteome of Patients with Hypothyroidism before and after Thyroid Hormone Replacement: A Proteomic Analysis. International journal of molecular sciences. 2018;19(1).
21. Wessel D, Flugge UI. A method for the quantitative recovery of protein in dilute solution in the presence of detergents and lipids. Analytical biochemistry. 1984;138(1):141-3.
22. Alfadda AA, Benabdelkamel H, Masood A, Moustafa A, Sallam R, Bassas A, et al. Proteomic analysis of mature adipocytes from obese patients in relation to aging. Experimental gerontology. 2013;48(11):1196-203.
23. Benabdelkamel H, Masood A, Almidani GM, Alsadhan AA, Bassas AF, Duncan MW, et al. Mature adipocyte proteome reveals differentially altered protein abundances between lean, overweight and morbidly obese human subjects. Molecular and cellular endocrinology. 2015;401:142-54.
24. Vall-Palomar M, Arevalo J, Ariceta G, Meseguer A. Establishment of urinary exosome-like vesicles isolation protocol for FHHNC patients and evaluation of different exosomal RNA extraction methods. Journal of translational medicine. 2018;16(1):278.
25. Hennemann G, Krenning EP, Docter R. Thyroid Hormone-Binding Plasma Proteins. In: Medeiros-Neto G, Gaitan E, editors. Frontiers in Thyroidology: Volume 1. Boston, MA: Springer US; 1986. p. 97-101.
26. Alfadda AA, Turjoman AA, Moustafa AS, Al-Naami MY, Chishti MA, Sallam RM, et al. A proteomic analysis of excreted and circulating proteins from obese patients following two different weight-loss strategies. Exp Biol Med (Maywood). 2014;239(5):568-80.

27. Turemen EE, Cetinarslan B, Sahin T, Canturk Z, Tarkun I. Endothelial dysfunction and low grade chronic inflammation in subclinical hypothyroidism due to autoimmune thyroiditis. Endocrine journal. 2011;58(5):349-54.
28. Rao PV, Lu X, Standley M, Pattee P, Neelima G, Girisesh G, et al. Proteomic identification of urinary biomarkers of diabetic nephropathy. Diabetes care. 2007;30(3):629-37.
29. Lin KH, Lee HY, Shih CH, Yen CC, Chen SL, Yang RC, et al. Plasma protein regulation by thyroid hormone. The Journal of endocrinology. 2003;179(3):367-77.
30. Southwell BR, Duan W, Alcorn D, Brack C, Richardson SJ, Kohrle J, et al. Thyroxine transport to the brain: role of protein synthesis by the choroid plexus. Endocrinology. 1993;133(5):2116-26.
31. Benabdelkamel H, Masood A, Alanazi IO, Alfadda AA. Comparison of protein precipitation methods from adipose tissue using difference gel electrophoresis. Electrophoresis. 2018.
32. Hara-Kuge S, Ohkura T, Seko A, Yamashita K. Vesicular-integral membrane protein, VIP36, recognizes high-mannose type glycans containing alpha1-->2 mannosyl residues in MDCK cells. Glycobiology. 1999;9(8):833-9.
33. Kim PS, Arvan P. Folding and assembly of newly synthesized thyroglobulin occurs in a pre-Golgi compartment. The Journal of biological chemistry. 1991;266(19):12412-8.
34. Zhang Q, Skepper JN, Yang F, Davies JD, Hegyi L, Roberts RG, et al. Nesprins: a novel family of spectrin-repeat-containing proteins that localize to the nuclear membrane in multiple tissues. Journal of cell science. 2001;114(Pt 24):4485-98.
35. Jevtic P, Levy DL. Nuclear size scaling during Xenopus early development contributes to midblastula transition timing. Current biology : CB. 2015;25(1):45-52.
36. Rajgor D, Shanahan CM. Nesprins: from the nuclear envelope and beyond. Expert reviews in molecular medicine. 2013;15:e5.
37. Chen S, Dong H, Yang S, Guo H. Cathepsins in digestive cancers. Oncotarget. 2017;8(25):41690-700.
38. Weber J, McInnes J, Kizilirmak C, Rehders M, Qatato M, Wirth EK, et al. Interdependence of thyroglobulin processing and thyroid hormone export in the mouse thyroid gland. European journal of cell biology. 2017;96(5):440-56.
39. Dunn AD, Crutchfield HE, Dunn JT. Thyroglobulin processing by thyroidal proteases. Major sites of cleavage by cathepsins B, D, and L. The Journal of biological chemistry. 1991;266(30):20198-204.
40. Liaudet-Coopman E, Beaujouin M, Derocq D, Garcia M, Glondu-Lassis M, Laurent-Matha V, et al. Cathepsin D: newly discovered functions of a long-standing aspartic protease in cancer and apoptosis. Cancer letters. 2006;237(2):167-79.
41. Jia Y, Hao S, Jin G, Li H, Ma X, Zheng Y, et al. Overexpression of ARNT2 is associated with decreased cell proliferation and better prognosis in gastric cancer. Molecular and cellular biochemistry. 2019;450(1-2):97-103.
42. Webb EA, AlMutair A, Kelberman D, Bacchelli C, Chanudet E, Lescai F, et al. ARNT2 mutation causes hypopituitarism, post-natal microcephaly, visual and renal anomalies. Brain : a journal of neurology.

2013;136(Pt 10):3096-105.
43. Citterio CE, Veluswamy B, Morgan SJ, Galton VA, Banga JP, Atkins S, et al. De novo triiodothyronine formation from thyrocytes activated by thyroid-stimulating hormone. The Journal of biological chemistry. 2017;292(37):15434-44.
44. Saber-Lichtenberg Y, Brix K, Schmitz A, Heuser JE, Wilson JH, Lorand L, et al. Covalent cross-linking of secreted bovine thyroglobulin by transglutaminase. FASEB journal : official publication of the Federation of American Societies for Experimental Biology. 2000;14(7):1005-14.
45. Zabczynska M, Kozlowska K, Pochec E. Glycosylation in the Thyroid Gland: Vital Aspects of Glycoprotein Function in Thyrocyte Physiology and Thyroid Disorders. International journal of molecular sciences. 2018;19(9).
46. Hosokawa N, Kamiya Y, Kamiya D, Kato K, Nagata K. Human OS-9, a lectin required for glycoprotein endoplasmic reticulum-associated degradation, recognizes mannose-trimmed N-glycans. The Journal of biological chemistry. 2009;284(25):17061-8.
47. Lee IH, Song SH, Cook DI, Dinudom A. H-Ras mediates the inhibitory effect of epidermal growth factor on the epithelial Na+ channel. PloS one. 2015;10(3):e0116938.
48. Dou R, Zhang L, Lu T, Liu D, Mei F, Huang J, et al. Identification of a novel HRAS variant and its association with papillary thyroid carcinoma. Oncology letters. 2018;15(4):4511-6.
49. Lemoine NR, Mayall ES, Wyllie FS, Williams ED, Goyns M, Stringer B, et al. High frequency of ras oncogene activation in all stages of human thyroid tumorigenesis. Oncogene. 1989;4(2):159-64.
50. Namba H, Gutman RA, Matsuo K, Alvarez A, Fagin JA. H-ras protooncogene mutations in human thyroid neoplasms. The Journal of clinical endocrinology and metabolism. 1990;71(1):223-9.
51. James MA, Vikis HG, Tate E, Rymaszewski AL, You M. CRR9/CLPTM1L regulates cell survival signaling and is required for Ras transformation and lung tumorigenesis. Cancer research. 2014;74(4):1116-27.

Tables

Table 1. Biochemical parameters of the study subjects at baseline and after L-thyroxine therapy.

	Hypothyroid	Euthyroid	*p*-value
N	9 (6 f)	9 (6 f)	
Age (years)	39.3 ± 12.9	39.3 ± 12.9	
Fasting glucose (mmol/L)	5.3 ± 0.4	5.0 ± 0.5	0.078
Urea (mmol/L)	4.7 ± 0.7	4.6 ± 0.9	0.392
Creatinine (mmol/L)	72.5 ± 13.1	76.1 ± 23.3	0.404
Aspartate transaminase (IU/L)	33.4 ± 6.6	37.5 ± 9.0	0.407
Alanine transaminase (IU/L)	18.0 ± 5.8	17.4 ± 3.9	0.169
Alkaline phosphatase (IU/L)	94.9 ± 25.9	96.8 ± 31.2	0.133
FT4 (pmol/L)	8.3 ± 5.5	18.8 ± 3.7	0.000
TSH (mIU/l)	33.9 ± 22.1	1.6 ± 0.9	0.000
Total Cholesterol (mmol/L)	4.6 ± 0.6	4.8 ± 0.7	0.193
Triglycerides (mmol/L)	1.2 ± 0.3	1.4 ± 0.3	0.184
LDL cholesterol (mmol/L)	2.9 ± 0.8	3.0 ± 0.6	0.373
HDL cholesterol (mmol/L)	1.2 ± 0.4	1.0 ± 0.3	0.087

Table 2: Identified proteins, with changes in abundance of significantly differentially abundant proteins between hypothyroid and euthyroid states in urine samples. Table 2 shows values for the average ratio between the two states, with their corresponding levels of fold changes and one-way ANOVA (p-value < 0.05) using 2D-DIGE. [Analysis type: MALDI-TOF; database: SwissProt; taxonomy: Homo sapiens].

ɔot ·o[a]	Accession No[b]	Protein Name	MASCOT ID	*P*-Value (ANOVA)	Ratio Hypo\Euth	EXP[f]
76	P02768	Serum albumin	ALBU_HUMAN	0.009	1.9	UP
56	P02768	Serum albumin	ALBU_HUMAN	0.015	2.8	UP
00	O75409	Huntingtin-interacting protein M	HYPM_HUMAN	0.002	3.3	UP
17	P02787	Serotransferrin	TRFE_HUMAN	0.044	4.5	UP
42	P21281	V-type proton ATPase subunit B, brain isoform	VATB2_HUMAN	0.006	2.3	UP
43	O95395	Beta-1,3-galactosyl-O-glycosyl-glycoprotein beta-1,6-N-acetylglucosaminyltransferase 3	GCNT3_HUMAN	0.028	2.8	UP
35	Q5T197	E3 ubiquitin-protein ligase DCST1	DCST1_HUMAN	0.014	2.4	UP
50	P07339	Cathepsin D	CATD_HUMAN	0.026	2.5	UP
19	Q8N806	Putative E3 ubiquitin-protein ligase UBR7	UBR7_HUMAN	0.008	1.9	UP
09	P13645	Keratin, type I cytoskeletal 10	K1C10_HUMAN	0.016	1.5	UP
08	Q8N7C3	Probable E3 ubiquitin-protein ligase TRIML2	TRIMM_HUMAN	0.036	1.5	UP
28	Q6FIF0	AN1-type zinc finger protein 6	ZFAN6_HUMAN	0.038	2.1	UP
28	Q6FIF0	AN1-type zinc finger protein 6	ZFAN6_HUMAN	0.039	1.8	UP
98	P13647	Keratin, type II cytoskeletal 5	K2C5_HUMAN	0.044	1.6	UP
34	P02760	Protein AMBP	AMBP_HUMAN	0.021	2.8	UP
02	Q12907	Vesicular integral-membrane protein VIP36	LMAN2_HUMAN	0.018	2.2	UP
98	P01042	Kininogen-1	KNG1_HUMAN	0.0015	1.8	UP

78	P02768	Serum albumin	ALBU_HUMAN	0.009	1.6	UP
18	Q8IZU9	Kin of IRRE-like protein 3	KIRR3_HUMAN	0.014	-3	DOWN
44	Q96CD2	Phosphopantothenoylcysteine decarboxylase	COAC_HUMAN	0.021	-2.3	DOWN
10	Q8NFX7	Syntaxin-binding protein 6	STXB6_HUMAN	0.042	-1.7	DOWN
81	O95395	Beta-1,3-galactosyl-O-glycosyl-glycoprotein beta-1,6-N-acetylglucosaminyltransferase 3	GCNT3_HUMAN	0.039	1.8	UP
50	O95395	Beta-1,3-galactosyl-O-glycosyl-glycoprotein beta-1,6-N-acetylglucosaminyltransferase 3	GCNT3_HUMAN	0.041	2.0	UP
08	Q9HBZ2	Aryl hydrocarbon receptor nuclear translocator 2	ARNT2_HUMAN	0.04	-2.1	DOWN
03	P01112	GTPase HRas	RASH_HUMAN	0.05	-2.2	DOWN
70	P02768	Serum albumin	ALBU_HUMAN	0.049	3	UP
55	Q8NF91	Nesprin-1	SYNE1_HUMAN	0.04	-3.4	DOWN
48	Q9UQ35	Serine/arginine repetitive matrix protein 2	SRRM2_HUMAN	0.006	-2.6	DOWN
35	Q8NF91	Nesprin-1	SYNE1_HUMAN	0.010	-2.5	DOWN
93	Q8NF91	Nesprin-1	SYNE1_HUMAN	0.016	-2.1	DOWN
47	Q6FIF0	AN1-type zinc finger protein 6	ZFAN6_HUMAN	0.016	-2.5	DOWN
52	Q96PF1	Protein-glutamine gamma-glutamyltransferase Z	TGM7_HUMAN	0.022	-3.9	DOWN
05	A6NJ69	IgA-inducing protein homolog	IGIP_HUMAN	0.023	-2.1	DOWN
04	Q9UP79	A disintegrin and metalloproteinase with thrombospondin motifs 8	ATS8_HUMAN	0.042	-1.9	DOWN

30	O15212	**Prefoldin subunit 6**	PFD6_HUMAN	0.030	-2.1	**DOWN**
56	Q96KA5	**Cleft lip and palate transmembrane protein 1-like protein**	CLP1L_HUMAN	0.021	1.7	**UP**
26	P02760	**Protein AMBP**	AMBP_HUMAN	0.022	2.4	**UP**
18	A8K0R7	**Zinc finger protein 839**	ZN839_HUMAN	0.026	2.5	**UP**
41	P02760	**Protein AMBP**	AMBP_HUMAN	0.052	2.1	**UP**
02	Q93099	**Homogentisate 1,2-dioxygenase**	HGD_HUMAN	0.053	1.6	**UP**
00	Q13438	**Protein OS-9**	OS9_HUMAN	0.058	1.9	**UP**
53	P02753	**Retinol-binding protein 4**	RET4_HUMAN	0.058	1.9	**UP**

[a] Protein accession number for SWISSPROT Database.

[b] Theoretical isoelectric point.

[c] Theoretical relative mass.

[d] MASCOT score

[e] Protein expression between hypothyroid and euthyroid states

Additional Files

Additional file 1: Figure S1: The power curve was used to calculate the sample size required to find significant difference with a fold-change of ≥1.5 between two paired groups at 98% power and p-value ≤ 0.05

Additional file 1: Figure S2. The figure shows the different canonical pathways obtained from IPA functional analysis.

Additional file 1: Table S1. Experimental design**:** 18 samples run on 9 2D-PAGE gels, samples were labeled randomly with Cy3 and Cy5, and a pooled sample was used as an internal standard and was stained with Cy2

Additional file 1: Table S2. Mass spectrometry analysis**:** Mass spectrometry list of significant differentially abundant proteins between Hypo and Euth identified in urine samples, using 2D-DIGE with. Protein name, accession number, Mascot score, MS % coverage, protein MW and pI values according to Uniprot database are listed.

Figures

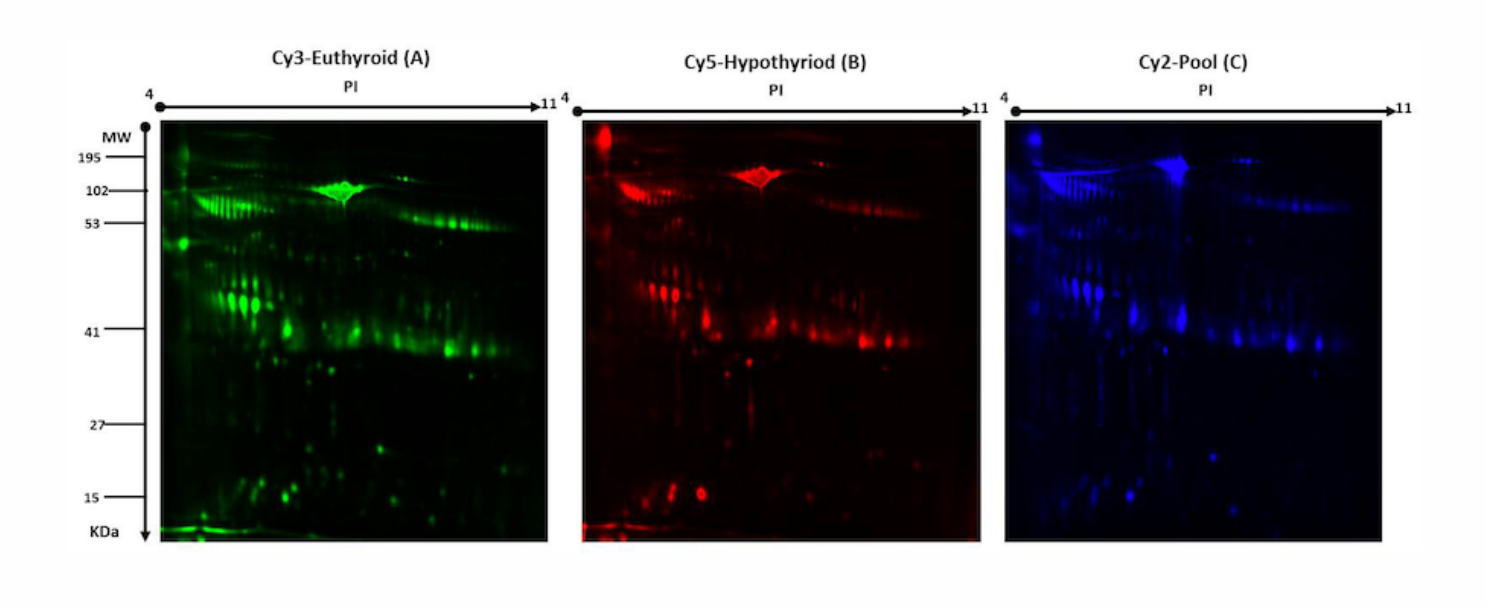

Figure 1

2D-DIGE analysis and identification of differentially expressed proteins. Representative fluorescent protein profiles of a 2D-DIGE containing - euthyroid samples labelled with Cy3 (A), hypothyroid labelled with Cy5 (B) and pooled internal control labelled with Cy2 (C). Urine proteins were separated on IPG strip (pH 3–11) in the first dimension followed by 12.5% PAGE in the second-dimension gel electrophoresis. Images were captured using a Typhoon 9400 Variable Mode Image

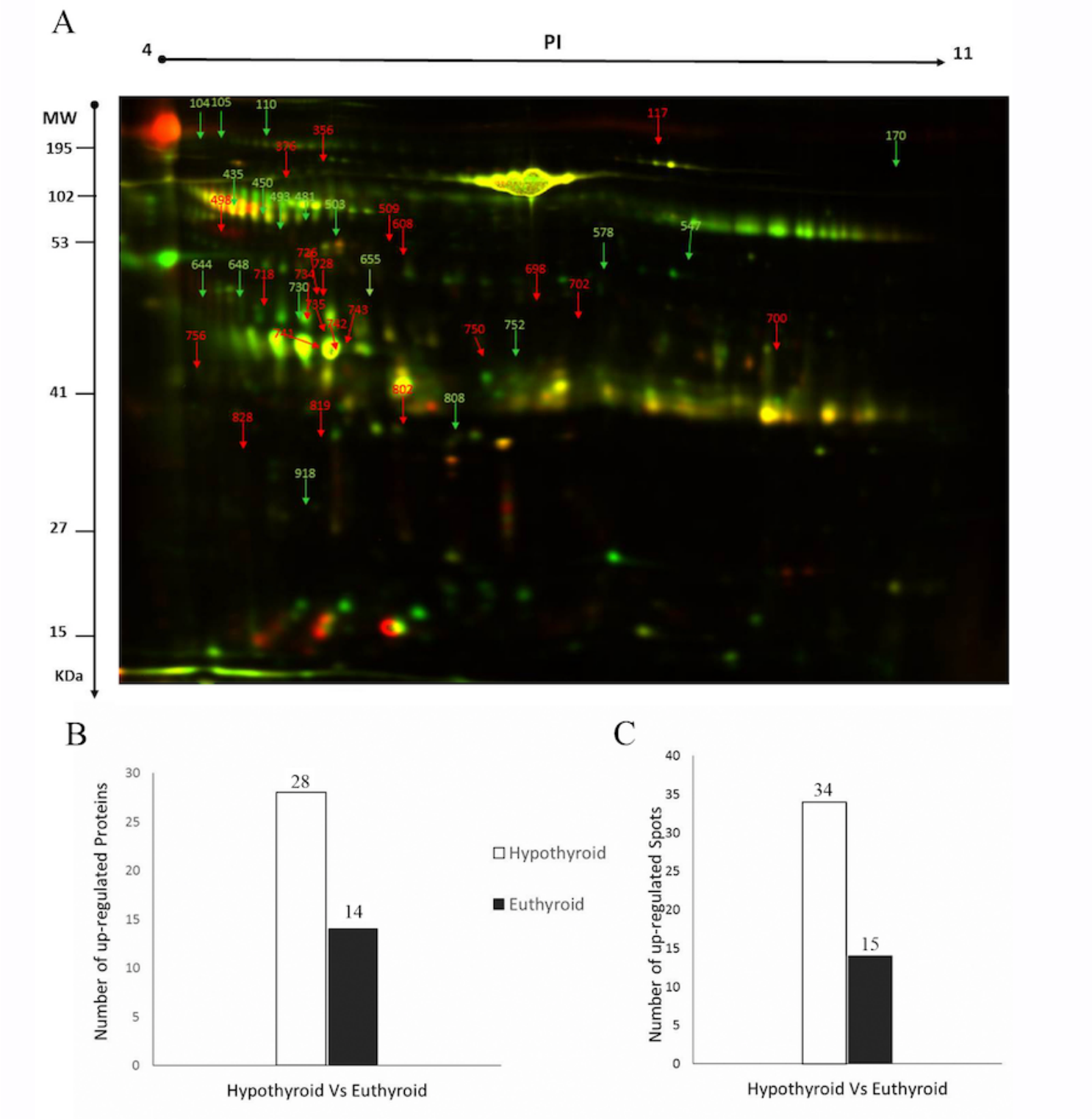

Figure 2

Representative image of gel depicting the protein spots identified with MALDI-TOF/TOF in the urine samples. Numbered spots indicate those which were significantly differentially abundant (over 1.5-fold change, $p < 0.05$) (A) between hypothyroid and euthyroid states. The red and green arrows indicate the differentially abundant proteins that are up-regulated and down-regulated respectively between the two

states. Graph showing the number of proteins successively identified by MALDI-TOF (B) and the number of statistical significantly upregulated spots in the hypothyroid compared to the euthyroid state (C).

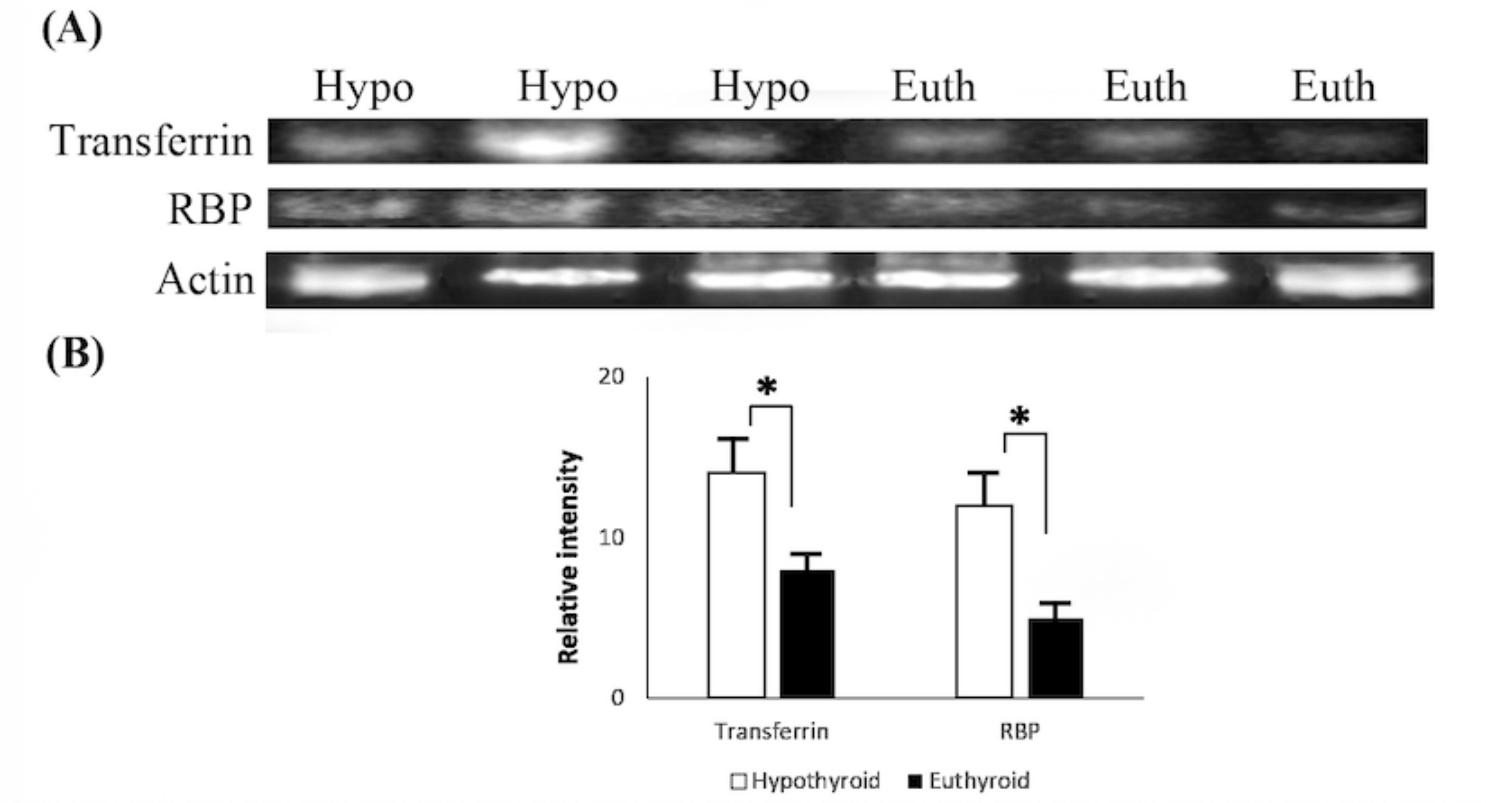

Figure 3

Confirmation of the proteomic data using immunoblot analysis of selected proteins, identified by 2-DE analysis. Results obtained by immunoblotting were similar to the results obtained by 2D-DIGE (A). Graphical representation of the relative intensity values of normalized protein bands between the hypothyroid and euthyroid states. The data are reported as histograms of the mean ± SD (B).

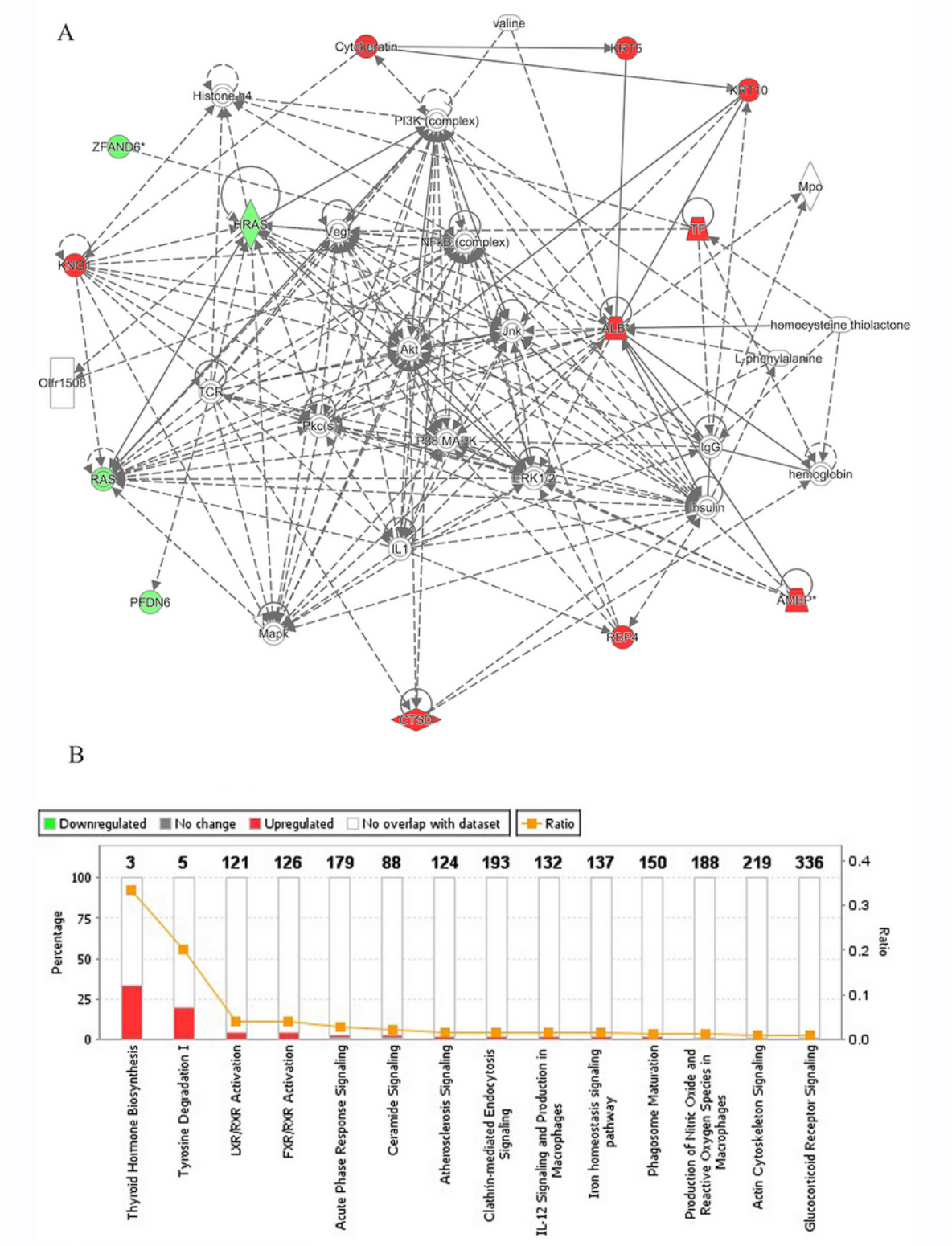

Figure 4

The most enriched interaction network of the differentially expressed proteins in hypothyroid compared to the euthyroid states. Red nodes indicate up-regulated; green nodes indicate down-regulated. The central nodes of the pathway related to signaling of the MAP kinases, Pkc, VEGF, PI3 kinase/Akt were found to be deregulated between the two states. Uncolored nodes are proposed by IPA and indicate potential targets that were functionally coordinated with the differentially expressed proteins. Solid lines indicate direct

molecular interactions, and dashed lines represent indirect interactions (A). The diagram showing the 14 top canonical pathways ranked by the P-values obtained by the IPA.

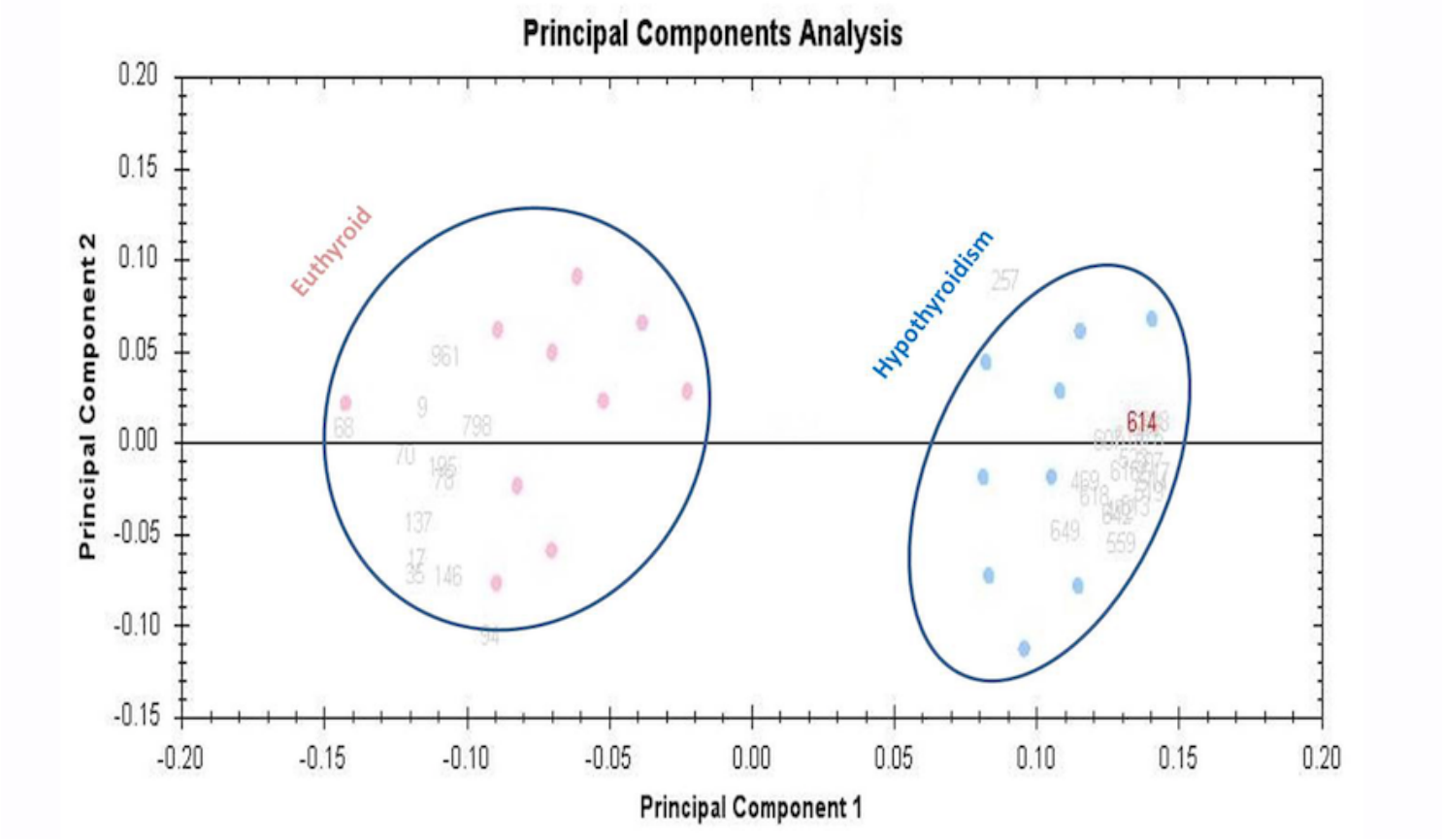

Figure 5

Principal component analysis of the proteomic dataset. Principal component analysis is presented in the figure where purple dots are the euthyroid and blue dots are the Hypothyroid. Both together these explained 64 % of the selected spot's variability values. Colored dots and numbers are the representation of gels and spots, respectively.

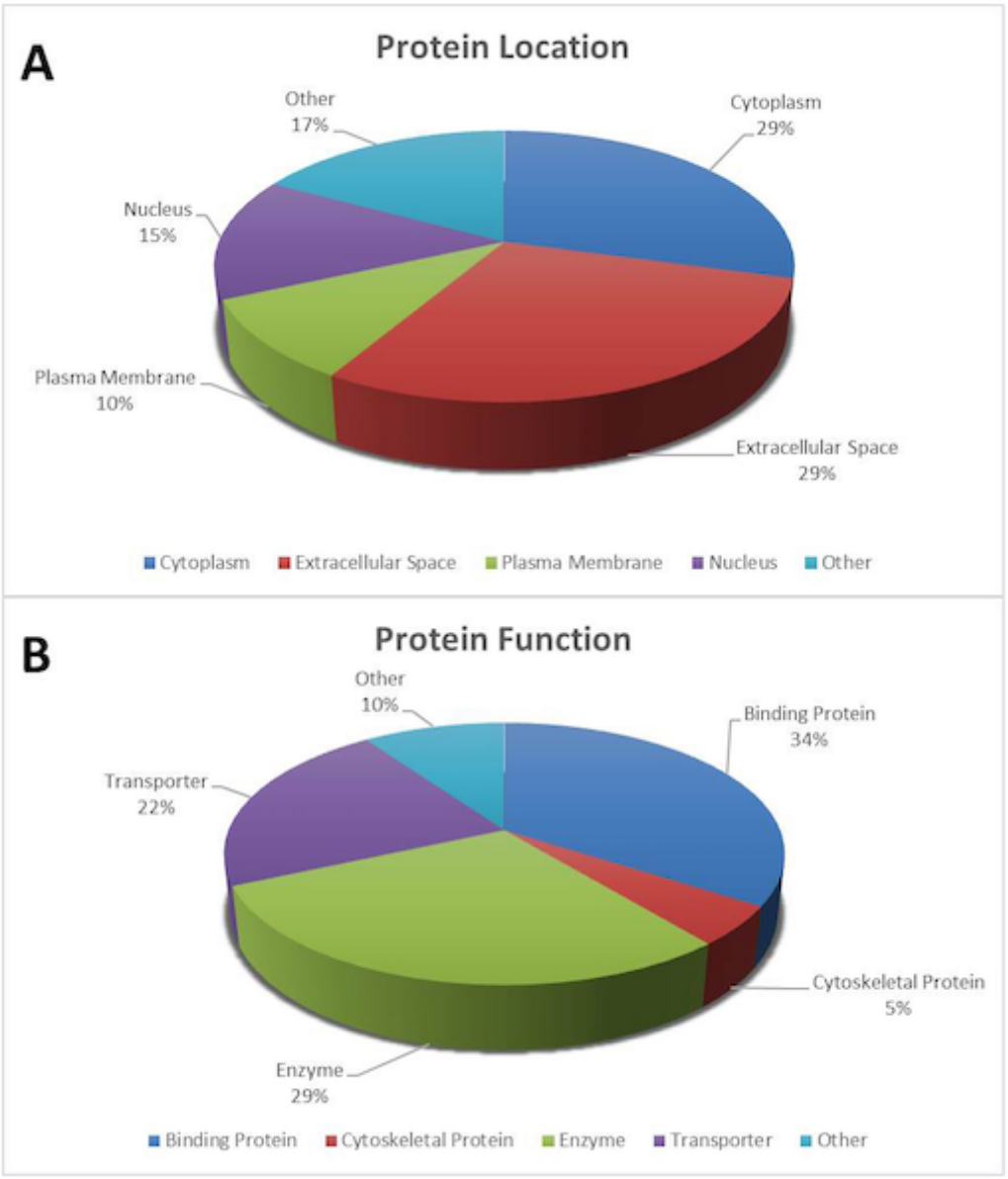

Figure 6

Comparative depiction (%) of the significantly identified proteins using MALDI-TOF/TOF-MS: categorized into groups according to their location (A), and function (B).

Supplementary Files

This is a list of supplementary files associated with this preprint. Click to download.

- Additionalfile.pdf